C-FGF23 peptide alleviates hypoferremia during acute inflammation

Rafiou Agoro,[1] Min Young Park,[1] Carole Le Henaff,[1] Stanislovas Jankauskas,[1] Alina Gaias,[1] Gaozhi Chen,[2] Moosa Mohammadi[3] and Despina Sitara[1,4]

[1]Department of Basic Science and Craniofacial Biology, NYU College of Dentistry, New York, NY, USA; [2]Chemical Biology Research Center, School of Pharmaceutical Sciences, Wenzhou Medical University, Wenzhou, China; [3]Departments of Biochemistry and Molecular Pharmacology, NYU School of Medicine, New York, NY, USA and [4]Department of Medicine, NYU School of Medicine, New York, NY, USA

 doi:10.3324/haematol.2019.237040

Received: September 2, 2019.

Accepted: March 13, 2020.

Pre-published: March 19, 2020.

Correspondence: *DESPINA SITARA* - ds199@nyu.edu

C-FGF23 peptide alleviates hypoferremia during acute inflammation

Rafiou Agoro[1], Min Young Park[1], Carole Le Henaff[1], Stanislovas Jankauskas[1], Alina Gaias[1], Gaozhi Chen[2], Moosa Mohammadi[3], Despina Sitara[1, 4, *]

Supplemental data

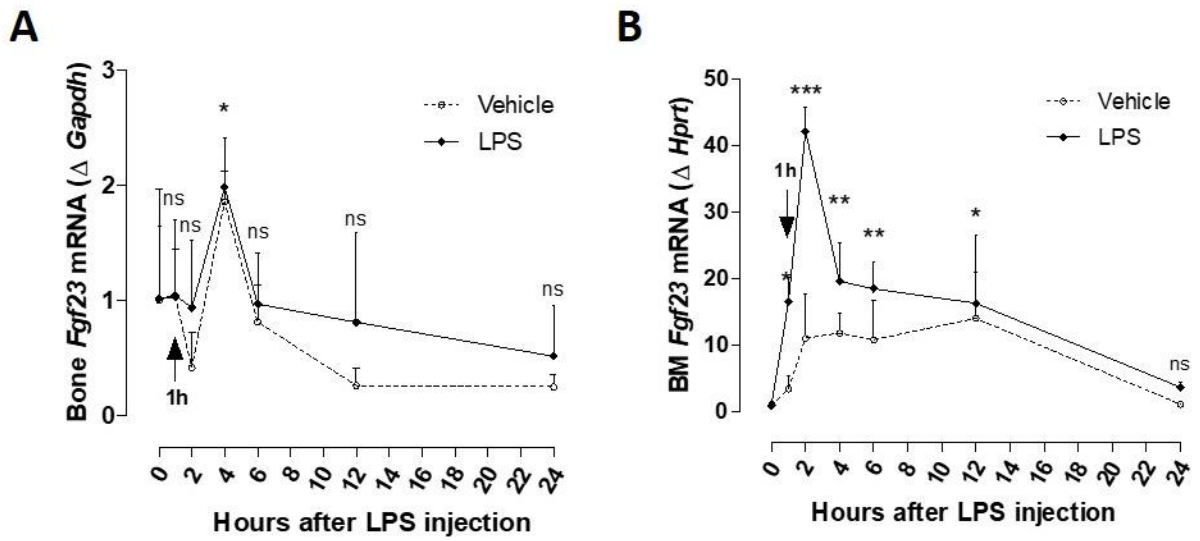

Suppl. Figure S1. Effect of LPS on *Fgf23* expression in bone and bone marrow.

C57BL/6J mice were injected i.p. with a single dose of saline (0.9% NaCl, indicated as Vehicle) or LPS (50 µg/kg). Samples were collected at 0, 1, 2, 4, 6, 12, and 24 hours after injection and total mRNA was isolated. Quantitative real-time RT-PCR for *Fgf23* expression in **(A)** bone, and **(B)** bone marrow (BM). Data are expressed as fold change ($2^{-\Delta\Delta Ct}$) relative to housekeeping genes *Gapdh* or *Hprt.* Samples were measured in duplicates (vehicle, n=3-4; LPS, n=5-8). Data are represented as mean +/- SD. All data were analyzed for normality by Shapiro-Wilk test and equivalence of variance using Levene's test. As the samples were not in normal distribution, data were analyzed with non-parametric Kruskal-Wallis test in each vehicle- or LPS-treated group compared to 0 h. ns: not significant compared to 0 h. *$P < 0.05$, **$P < 0.01$, ***$P < 0.001$ compared to 0 h.

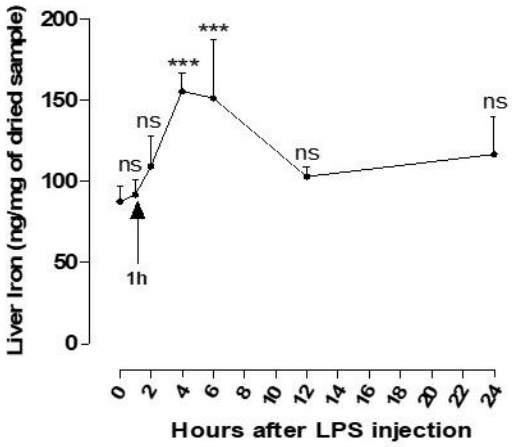

Suppl. Figure S2. Effect of LPS on liver iron content.

C57BL/6J mice were injected i.p. with a single dose of LPS (50 µg/kg). Samples were collected at 0, 1, 2, 4, 6, 12, and 24 hours after injection. Samples were measured in duplicates (n=3). Data are represented as mean +/- SD. All data were analyzed for normality by Shapiro-Wilk test and equivalence of variance using Levene's test, followed by one-way ANOVA with Bonferroni's multiple comparison test. ns: not significant compared to 0 h, ***$P < 0.001$ compared to 0 h.

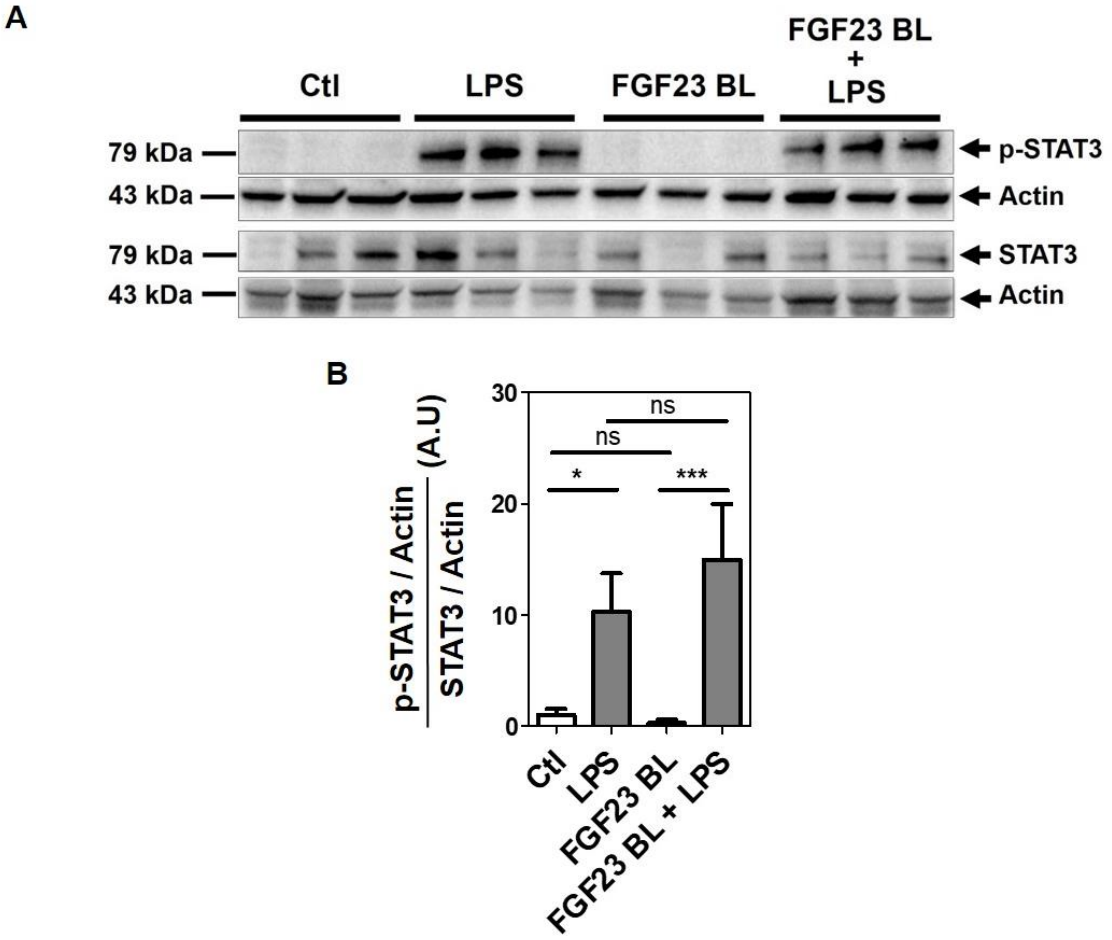

Suppl. Figure S3. Effect of inhibition of FGF23 signaling on STAT3 signaling in LPS-challenged mice.

C57BL/6J wild type mice were treated with C-tail FGF23 (1 mg/kg, indicated as FGF23 BL) or vehicle (HEPES buffer) for 8 hours. Mice were then challenged with LPS (i.p 50 µg/kg) or vehicle (0.9% NaCl) for 4 h. **(A)** Representative western blot image, and **(B)** ratio of phospho-STAT3 to STAT3 for 3 mice per each group. Data are expressed as ratio of STAT3 or phospho-STAT3 signal intensity to housekeeping protein (Actin) signal intensity in arbitrary units (A.U.). Data are represented as mean +/- SD. All data were analyzed for normality by Shapiro-Wilk test and equivalence of variance using Levene's test. Because data were not showing normal distribution, same tests were proceeded after data were aligned in rank transformation. Then two-way ANOVA was performed with Bonferroni's multiple comparison test. Ctl: control (vehicle), ns: not significant, **P* < 0.05, ****P* < 0.001.

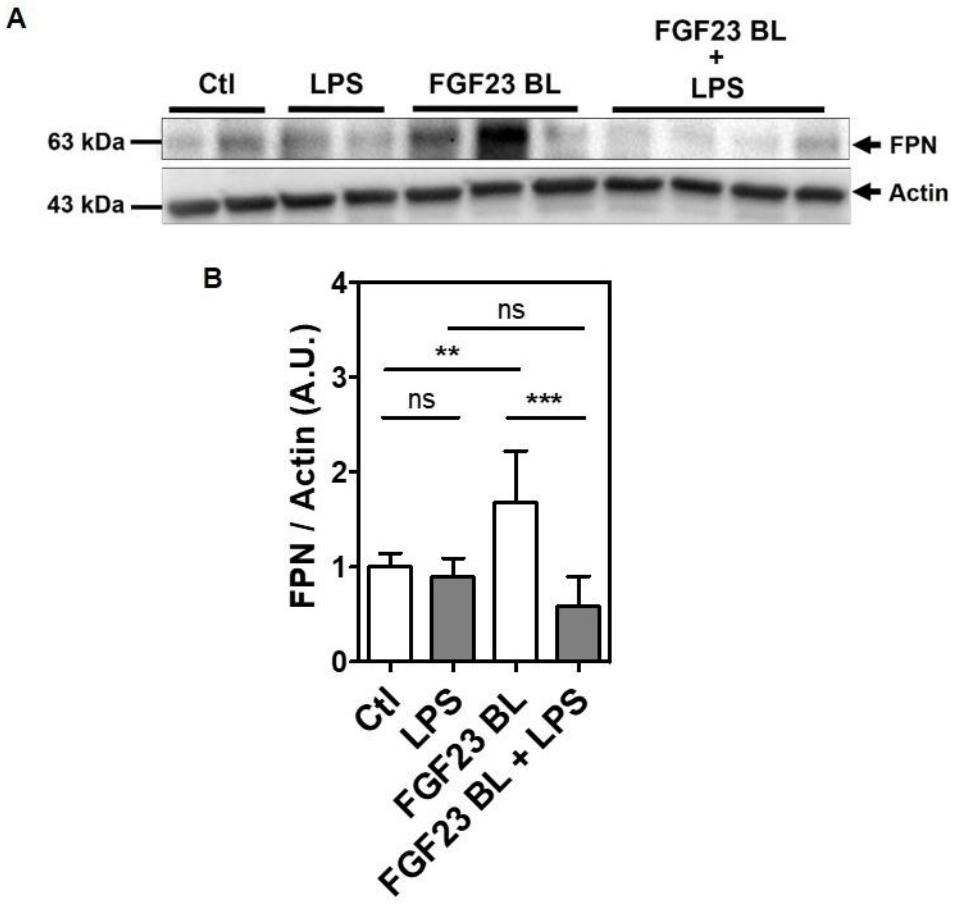

Suppl. Figure S4. Inhibition of FGF23 signaling increases spleen Ferropotrin (FPN) protein levels.

C57BL/6J wild type mice were treated with C-tail FGF23 (1 mg/kg, indicated as FGF23 BL) or vehicle (HEPES buffer) for 8 hours. Mice were then challenged with LPS (i.p 50 µg/kg) or vehicle (0.9% NaCl) for 4 h. **(A)** Representative western blot, and **(B)** calculated FPN abundance for two western blots comprising 3-5 mice per group. Data are expressed as ratio of FPN signal intensity to housekeeping protein (Actin) signal intensity in arbitrary units (A.U.). Data are represented as mean +/- SD. All data were analyzed for normality by Shapiro-Wilk test and equivalence of variance using Levene's test, followed by two-way ANOVA which was performed with Bonferroni's multiple comparison test. Ctl: control (vehicle) ns: not significant, $^{**}P < 0.01$, $^{***}P < 0.001$.

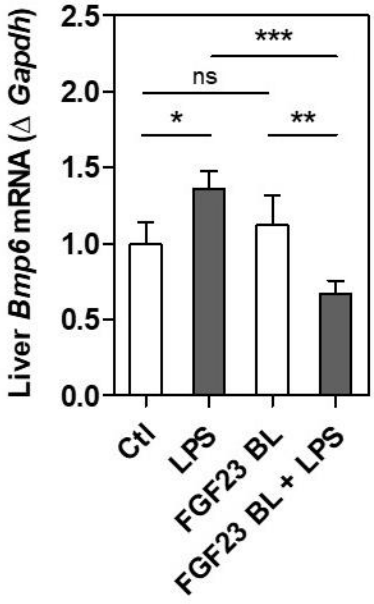

Suppl. Figure S5. Effect of FGF23 signaling inhibition on hepatic *Bmp6* mRNA expression
C57BL/6J wild type mice were treated with C-tail FGF23 (1 mg/kg, indicated as FGF23 BL) or vehicle (HEPES buffer) for 8 hours. Mice were then challenged with LPS (i.p 50 µg/kg) or vehicle (0.9% NaCl) for 4 h. Quantitative real-time RT-PCR for hepatic expression of *Bmp6*. Data are expressed as fold change ($2^{-\Delta\Delta Ct}$) relative to housekeeping gene *Gapdh*. Samples were measured in duplicates (n=5-7 per group). Data are represented as mean +/- SD. All data were analyzed for normality by Shapiro-Wilk test and equivalence of variance using Levene's test, followed by two-way ANOVA with Bonferroni's multiple comparison test. Ctl: control (vehicle) ns: not significant, **P* < 0.05, ***P* < 0.01, ****P* < 0.001.

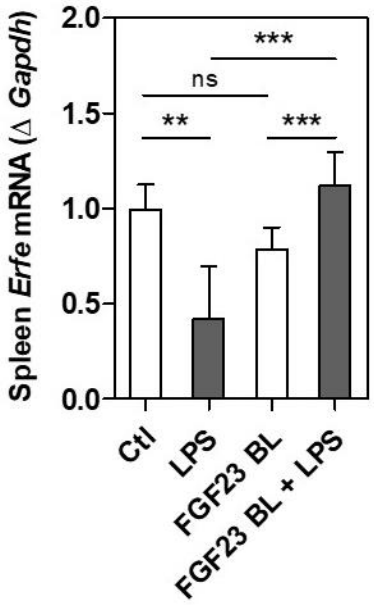

Suppl. Figure S6. Effect of FGF23 signaling inhibition on splenic *Erfe* mRNA expression

C57BL/6J wild type mice were treated with C-tail FGF23 (1 mg/kg, indicated as FGF23 BL) or vehicle (HEPES buffer) for 8 hours. Mice were then challenged with LPS (i.p 50 µg/kg) or vehicle (0.9% NaCl) for 4 h. **(A-C)** Quantitative real-time RT-PCR for splenic expression of *Erfe*. Data are expressed as fold change ($2^{-\Delta\Delta Ct}$) relative to housekeeping gene *Gapdh*. Samples were measured in duplicates (n=5-7 per group). Data are represented as mean +/- SD. All data were analyzed for normality by Shapiro-Wilk test and equivalence of variance using Levene's test. As the samples were not in normal distribution, data were analyzed with non-parametric Kruskal-Wallis test. Ctl: control (vehicle), ns: not significant, $^{**}P < 0.01$, $^{***}P < 0.001$.

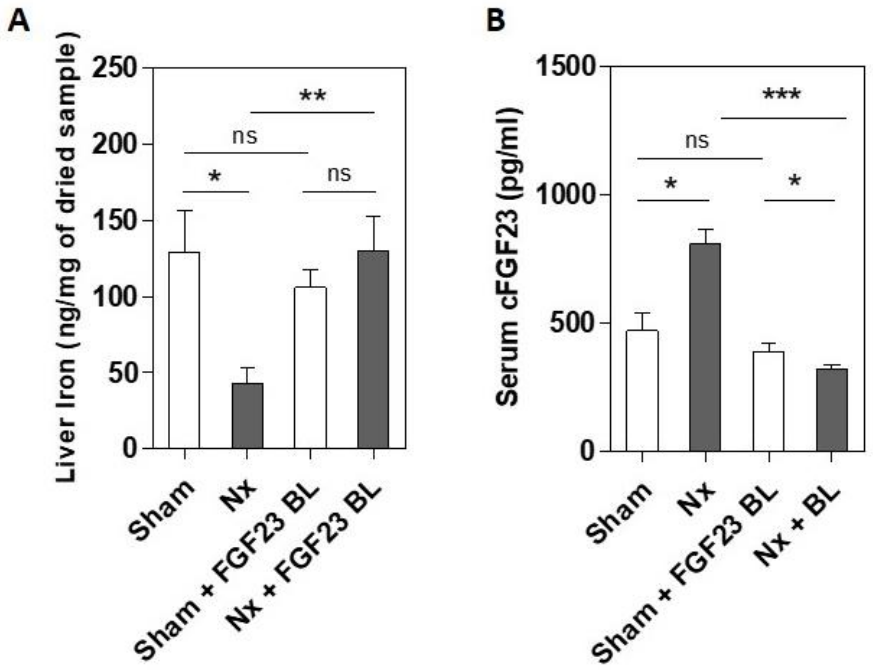

Suppl. Figure S7. Effect of FGF23 signaling inhibition on liver iron content and serum FGF23 in a mouse model of chronic kidney disease.

Control (Sham) and 5/6 nephrectomy (Nx) mice of 18 weeks of age were injected i.p. with the C-tail FGF23 (10 mg/kg, indicated as FGF23 BL) or vehicle (HEPES buffer) and evaluated 12 hours post-injection. **(A)** Liver iron content was measured using the Ferrozine assay, and **(B)** C-terminal FGF23 (cFGF23) was measured by ELISA. Samples were measured in duplicates. n = 6 mice per group. Data are presented as mean +/- SD. All data were analyzed for normality by Shapiro-Wilk test and equivalence of variance using Levene's test. As the samples showed normal distribution, two-way ANOVA was performed with Bonferroni's multiple comparison test (A). For data not showing normal distribution, same tests were proceeded after data were aligned in rank transformation. Then two-way ANOVA was performed in each vehicle- or LPS-treated group with Bonferroni's multiple comparison test (B). ns: not significant, $*P < 0.05$, $**P < 0.01$, $***P < 0.001$.

Supplementary Table 1

Gene	Primer	Sequence (5' - 3')
IL-6	Forward primer	ATC CAG TTG CCT TCT TGG GAC TGA
	Reverse primer	TAA GCC TCC GAC TTG TGA AGT GGT
TNF-α	Forward primer	AAG GGA GAG TGG TCA GGT TGC C
	Reverse primer	CCT CAG GGA AGA GTC TGG AAA GG
IL-1β	Forward primer	CAG GAT GAG GAC ATG AGC ACC
	Reverse primer	CTC TGC AGA CTC AAA CTC CAC
Fgf23	Forward primer	ACT TGG CCT TTA TTA GCC GGG TCT
	Reverse primer	AGA TGG CCT CTT CCC TGT GTT CAA
Klotho	Forward primer	AAA TGG CTG GTT TGT CTC GGG AAC
	Reverse primer	TAT GCC ACT CGA AAC CGT CCA TGA
Hepcidin (Hamp)	Forward primer	CAC CAC CTA TCT CCA TCA ACA G
	Reverse primer	GTT GGT GTC TCT CTT CCT TCT C
Bmp6	Forward primer	GTG TGG GCC TCC GAA GAA
	Reverse primer	ACA CTC AGC TGG AGT CCC ATG T
Lcn2	Forward primer	CCA GTT CGC CAT GGT ATT TT
	Reverse primer	AGT CTT GGC GTA AGG GTT CA
Epo	Forward primer	TCT ACG TAG CCT CAC TTC ACT
	Reverse primer	ACC CGG AAG AGC TTG CAG AAA
EpoR	Forward primer	GGG CTG CAT GGA CAA ACT
	Reverse primer	GCC GCT TTG CTC TCA AAC TT
NaPi2a	Forward primer	GTG CCT CTG ATG CTG GCT TTC
	Reverse primer	CTG GAA CTC TGC ACC AGA ACT
NaPi2c	Forward primer	CTC ACC ATA CAT GCA GAG CTA GGA
	Reverse primer	TGC ATT TCT CAG ACT CCG GT
Hif2α	Forward primer	GGG AAC ACT ACA CCC AGT GC
	Reverse primer	TCT TCA AGG GAT TCT CCA AGG
FtH	Forward primer	AAG TGC GCC AGA ACT ACC AC
	Reverse primer	CAG AGC CAC ATC ATC TCG GT
Fpn	Forward primer	CTC TGT CAG CCT GCT GTT TG
	Reverse primer	TCA GGA TTT GGG GCC AAG ATG
Hprt	Forward primer	AAG CCT AAG ATG AGC GCA AG
	Reverse primer	TTA CTA GGC AGA TGG CCA CA
Gadph	Forward primer	GAC TGT GGA TGG CCC CTC TG
	Reverse primer	CGC CTG CTT CAC CAC CTC CT